DESIGN AND PERFORMANCE OF A MULTI-STAGE CYLINDRICAL RECONNECTION LAUNCHER*

SAND--89-2112C

DE90 007820

Ronald J. Kaye, Edwin L. Brawley,** Billy W. Duggin, Eugene C. Cnare, Dean C. Rovang, and Melvin M. Widner
Sandia National Laboratories
Albuquerque, New Mexico 87185

Abstract

A multi-stage, cylindrical, reconnection launcher is being tested to demonstrate electrically-contactless, induction-launch technology for solenoidal coil geometry. A 6-stage launcher system is being developed to accelerate a 5 kg mass from rest to 300 m/s with a stored energy of ≥ 200 kJ per coil stage. This launcher will provide data for model verification and the engineering basis for proceeding with larger multi-stage systems.

This paper describes the design of the multi-stage, discrete-coil launcher. Integration of coils, projectile, power systems, and real-time fire control are discussed. Results of multi-stage firings are presented.

Introduction

Sandia National Laboratories is investigating the feasibility of using electromagnetic induction propulsion for launching small satellites into low Earth orbit. Our program is studying the concept of an Earth-to-Orbit (ETO) launcher which would accelerate a 1 metric ton launch package to 4 km/s at the Earth's surface to put a 70 kg payload into orbit. The basis for this concept stems from our development of system models to predict performance and the demonstration of induction

* This work supported by the U.S. Department of Energy with SNL under contract DE-AC04-76-DP00789.

** Rockwell Power Systems

---

launch technology with the 6-stage prototype cylindrical launcher discussed in this paper.

This prototype cylindrical launcher is not our first experience with induction launch technology. Our initial experiments were with a three-stage system using cylindrical geometry [1]. Our reconnection launcher evolved using a geometry where the magnetic field is orthogonal to the direction of projectile motion. The magnetic field lines 'reconnected' from a geometry of closed lines surrounding isolated coils to coupled lines which accelerated a plate projectile [2]. Our 14-stage reconnection launcher accelerated a 160 gram aluminum rectangular plate projectile to 1 km/s in August, 1988 [3]. During the testing of this launcher, we developed the computer modeling required to understand the control of projectile heating and predict performance [4].

The goal of our current work with the prototype cylindrical launcher is to demonstrate multi-stage induction launch capability in a cylindrical geometry with acceptable projectile heating using some of the technology developed in our previous launchers. This system will provide model verification and the engineering basis for proceeding with larger systems.

The Prototype Cylindrical Launcher is an induction type of linear motor. The operating sequence for a single stage of this type of device is shown in Figure 1.

Figure 1

1. Operation sequence for a single stage of an induction launcher.

Frame 1 of this figure shows the necessary components; a stator coil and a conducting armature which is the projectile. In our system, the

armature can be considered a single turn coil with a non-uniform eddy current distribution. The projectile enters the coil with an initial velocity from the left. This initial velocity is not fundamentally necessary to the operation of a single stage but is included here for illustration of any arbitrary stage of a multi-stage system. At this position there is no current in the coil, and the velocity of the projectile is measured by the firing system.

When the projectile reaches the position shown in frame 2, current is switched to the coil from a capacitor bank, generating a magnetic field between the coil and projectile. The pulsed field also generates an induced current in the projectile, which interacts with the field, producing a J x B Lorentz force accelerating the projectile out of the coil. The rise time of the coil and capacitor bank circuit is chosen such that the projectile is at a position as shown in frame 3 at the time of peak current resulting in maximum acceleration. With this geometry of coil and armature, the projectile continues to be accelerated until it decouples from the coil at a position shown in frame 4. In a multi-stage system, the projectile would be located in the next coil and the process repeated. In general, the projectile carries a persistent current into the next coil, which must be considered in the operation of the next stage.

The operating principle is modeled in our simulation code WARP-10 by a self-consistent electrical circuit analysis which includes equations of motion and material equations of state [4]. Figure 2 illustrates several launcher coils, each energized by a capacitor bank. The projectile is shown here as a single moving resistive coil coupled to the stator. However, in WARP-10, it is represented by many coupled loop circuits. After solving a system of loop equations for coil and armature currents, the forces, net acceleration, and Ohmic heating are calculated.

Figure 2

2. Circuit representation of several coil stages of a multi-stage launcher.

In a multi-stage system, coils are stacked end-to-end and energized sequentially, each providing an impulse to the projectile. In general, more than one coil is accelerating the projectile at any given time. WARP-10 includes the coupling of coils to each other and to the projectile.

Launcher Coils

Our design criteria included requirements for ease of fabrication, using available technology and hardware, flexibility in the design process, and capability of integration into a multi-stage launcher. The primary requirement was to accelerate 5 kg to 300 m/s. Another constraint was that the projectile outer diameter was fixed at 14 cm for possible application in another project. Calculations indicate that this can be accomplished in a 5-stage launcher with the capacitor bank of each stage storing 230 kJ of energy.

For convenience and rapid turnaround of modifications during the design process, we proposed winding coils of square magnet wire. The coil build was limited to two layers to minimize distortion of the windings. The length was determined by the requirement of having enough wire to keep the equilibrated, conductor-temperature rise below insulation limits. For ease of simulation and interchangeability of coils, we chose to use the same coil in each stage. However, this requires that we vary the capacitance of the bank of each stage.

The above criteria yielded a 2-layer, 38-turn coil winding of #4 square magnet wire. The three main design issues for the coil are

mechanical stress due to magnetic pressure, temperature distribution in the windings, and electrical stress of insulation.

Mechanical loads and distributions on the coil in the presence of the projectile were evaluated with finite-element field and circuit analysis models. Figure 3 shows the loads calculated by WARP-10 on the fourth stage coil winding at time of peak current of the capacitor discharge. The load vectors centered on the wires represent the applied pressure on each turn due to other coil currents and the projectile currents. Vectors at the edge of the winding represent the net pressures the winding exerts on the containment structure. Finite-element field analysis indicated the current distributions in the winding.

Figure 3

3. Calculated pressure on a coil winding at peak current while accelerating a projectile.

From the calculated loads, we determined the structure required to contain the radial and axial forces on the winding. The coil winding is captured in an assembly as shown in Figure 4. Radial loads are transferred through split rings to a coil support structure. Plates at the ends of the winding capture the axial reaction loads on the coil due to projectile acceleration. These endplates are held in place by externally compressing them axially against the split ring. The endplates also support a dielectric flyway tube which guides the projectile. The close-tolerance outer diameter of the split rings and endplates serve to align the flyway and coils.

Figure 4

4. Two layer coil winding in an assembly.

Figure 5

5. Coil assembly with fiberoptic component cassette and a 3.6 kg projectile.

Figure 5 shows notches cut radially in the endplates to form a channel providing access to the flyway for the optics of the firing system. The flyway is removed to illustrate the coil windings. The 3.6 kg aluminum projectile shown is described below.

The finished coil assembly has the following parameters:

38	turns in 2 layers
14.7	cm winding inner diameter
10.7	cm winding length
13.5	cm assembly length
166	≈H coil inductance without projectile
66	≈H coil inductance with projectile centered

Electrical insulation for the winding is compatible with the mechanical loads and the 110 ^{o}C estimated temperature rise of the windings using a 200 kJ energy store. We experimentally evaluated the dielectric breakdown strength of the wire insulation in the coil geometry with varying degrees of wire deformation.

We evaluated our prototype coil designs in a single-stage testbed by accelerating 5 kg, 14 cm OD, 20.3 cm length, 7075-T73 aluminum projectiles similar to that shown in Figure 5. A 20.5 mF capacitor bank storing energies up to 300 kJ energized the coil. With this testbed we evaluated coil and housing structural integrity, fiberoptic components

for the firing system, projectile mechanical integrity, and our simulation model. Shot rate was a few per hour.

For a typical 200 kJ test, the projectile was placed at rest with its rear surface near the coil midplane. The bank charged to 4.44 kV delivered 42 kA peak current to the coil generating a magnetic flux on the order of 18 Tesla in the annular gap between the coil and projectile. The projectile acceleration was determined using a VISAR interferometer (Velocity Interferometer System for Any Reflector) indicating a peak of 9 x 10^4 m/s^2 (9000 g's) and final velocity of 93 m/s [5]. This yields 11% of the initial stored energy converted to kinetic.

After 28 test firings in the energy range of 25 to 300 kJ, there was slight deformation to the winding due to axial forces, however the coil integrity was maintained. The tests showed the structure is sufficient to protect the fiberoptic components which are located between the coil assemblies. Comparison of performance predictions from our simulation model WARP-10 with data from these tests shows good agreement in Figure 6.

Figure 6

6. WARP-10 simulation predictions agree with single stage launcher test data.

Prototype Launcher Hardware

Figure 7 is a cutaway view of the 6-stage Prototype Cylindrical Launcher. Six of the coil assemblies described above are stacked end-to-end in a two-piece, stainless-steel support structure. The upper and lower halves form a cradle aligning the coil assemblies. The nominal

100 MPa (1 kbar) radial loads from the coils are transferred to the support housing through the split rings of the coil assembly. Insulated, tapered clamps are distributed along the length of the housings to hold the halves in place. The housing halves are insulated from one another to lengthen the paths of the induced eddy currents.

Figure 7

7. Cutaway view of the Prototype Cylindrical Launcher.

Axial loads from the coils are transferred to the endplates and split rings of the coil assembly, and ultimately to the large end clamps located at each end of the support housing. These end clamps, secured to the launcher base plate, provide axial compression on the stack of coils within the support housing. This minimizes movement of the coil assemblies during operation.

The endplates of each coil assembly hold a fiberglass (G10 grade) flyway tube coaxial with the coil windings for guiding the projectile through the launcher. Small holes cut in the flyway between the coil assemblies allow the light beams of the fiberoptic firing system to pass as chords across the path of the projectile.

The projectile is a 7075-T73 aluminum cylinder, 14 cm OD, 20.3 cm long, that has been partially hollowed out. Some projectiles are fitted with a nose to reduce drag during post-launch flight, but this is not required for launcher operation. Our projectile masses have ranged from 3 to 5 kg. Teflon bearing pads on the armature minimize the contact of the aluminum with the flyway tube.

Notches cut on the outside of the armature are used to spin the projectile in the breech prior to launch. This is done to provide

gyroscopic stability for the projectile during post-launch flight. Passing compressed air tangentially across the notches forms an air bearing in the breech spinner and causes the projectile to spin to rotational velocities of 150 revolutions per second.

The operating sequence is to spin the projectile while the capacitor banks are being charged. When full rotational velocity is reached, an air-driven piston pushes the spinning projectile into the first coil stage of the launcher. When the leading edge of the projectile reaches the fiberoptic cassette of the first stage, it interrupts two light beams separated by 7 mm. This timing information is used by the microprocessor-controlled firing system to determine the projectile velocity and the time delay required before triggering the capacitor bank switch to energize the coil [6]. The delay determined in real-time is the amount necessary for the projectile to reach the desired position in the coil at time of bank switch. This sequence is repeated in each of the coil stages.

Our simulation modeling of the launcher suggested that, for the coil design chosen, the half period of the capacitor bank discharge for any stage be on the order of the transit time of the projectile through the accelerating portion of the coil. Our point design was based on the velocity profile associated with accelerating a 5 kg projectile to 300 m/s with 230 kJ stored per stage. Since identical coils are used for every stage, we calculated the optimum capacitance and voltage of each stage for this energy level. Operation at lower acceleration will result in acceptable but non-optimum performance.

The criteria for capacitor selection could only be approximated with available capacitors. Therefore the bank for each coil stage is comprised of series and/or parallel combinations of 40-to-50 kJ rated capacitors. The capacitances of the banks are 20485, 5683, 2059, 1683, 835, and 684 ≈F for stages 1 to 6 respectively.

Charging each of the banks to a different initial voltage is simplified by an automatic charging system. At the beginning of the charge cycle, all the banks are connected to one of two power supplies. As the power supply voltages increase, computer controlled relays disconnect the bank of a stage when it reaches the desired charge. The bank waits in this condition, electrically isolated from the other capacitor banks, until triggered for discharge by the firing system during launch. The only connection between capacitor banks during launch is a single point ground at the launcher. The ground configuration is a star pattern centered at the midpoints of the launcher coils.

The capacitor banks are not generally charged to their full energy storage rating. Therefore, we allow the voltage to reverse during the discharge without significant loss of capacitor lifetime. The switches for discharging each of the capacitor banks into its coil are size D ignitrons. The banks in stages 1 through 3 are split into equal submodules, each with its own ignitron to handle the large coulomb transfer associated with the discharge of these stages.

Prototype Launcher Performance

Figures 8 and 9 illustrates the launcher elevated 15 degrees above horizontal prior to a shot. Much of the launcher hardware described in the above sections is visible.

Figure 8

8. Muzzle end of launcher.

Figure 9

9. Launcher elevated 15 degrees, ready for test.

The launcher tests conducted to date were with capacitor bank energies of 50 to 230 kJ/stage to characterize launcher performance. Our first goal was to reach a velocity milestone of 300 m/s with projectiles less than 5 kg mass to evaluate velocity effects. The stored energy was then increased to reach this velocity with a full mass projectile.

Shot 24 was designed to accelerate a 4.97 kg, cooled projectile to greater than 310 m/s. The 20.3 cm long, 14 cm OD, 7075-T73 projectile was hollowed out with a 15 mm wall thickness to a 14 cm depth from the front. Just prior to launch, the projectile was cooled with liquid nitrogen and loaded in the breech. The spinner was not used for this test to minimize the projectile temperature rise. The projectile warmed to -140 ^{o}C by the time the loader injected the projectile into the first stage at 11.9 m/s.

The following table indicates the shot performance. The quantities listed below by stage are the initial capacitor bank stored energy E_s, initial charge voltage V_o, peak coil current I_{pk}, projectile velocity v, kinetic energy increment associated with the velocity change ΔKE, and the efficiency, ε, which is the ratio $\Delta KE/E_s$. The projectile velocity listed with a given stage is measured during the operation of that stage. Since, in general, more than one coil is accelerating the projectile at a given time, this velocity is more a measure of system performance, rather than individual stage performance.

Stage #	E_s kJ	V_o kV	I_{pk} kA	v m/s	ΔKE kJ	ε %
1	214	4.6	30.8	80	15.5	7.2
2	233	9.1	31.0	145	36.4	15.7
3	223	14.7	43.7	226	73.9	33.1
4	223	16.3	40.7	274	59.9	26.8

5	162	19.7	41.3	307	48.6	29.9
6	141	20.3	41.5	335	44.2	31.4

The overall conversion of initial stored energy in the capacitors to projectile kinetic energy was 23.3%. The average acceleration of the projectile through the 81 cm length of the coil region of the launcher is 6.9×10^4 m/s^2 (6900 g's).

Figure 10 shows a comparison of the projectile velocity from each stage in shot 24 with calculations of velocity at the same location by our simulation model, WARP-10. Comparison is also made for shot 13 in which each of the 6 capacitor banks stored an average of 104 kJ to accelerate a 3.6 kg projectile.

Figure 10

10. Prototype Cylindrical Launcher data compared with WARP-10 simulations.

Modifications to the original code were necessary to include the effect of eddy currents in the housings which reduce the performance. The justification for inclusion of the housing inductive and resistive effects is based on finite-element field analysis of eddy current distributions and measurements of the coupling. A general analysis of the housing as a coupled distribution of circuits is not practical at this time.

Video coverage at the launcher muzzle showed the projectile in good condition as it exited the launcher. We recovered the projectile 550 m down range. Although damaged from impact, measurements of undamaged regions indicate no deformation of the armature from launch.

The projectile makes intermittent contact with the flyway during launch, which causes some flyway abrasion. This is apparently due to an imbalance of radial forces in the coils. No attempt was made during the launcher design to balance all radial forces or levitate the projectile. Shot rate is currently limited by data analysis and hardware inspection to one per day, but could be increased to 2-3 per day.

Summary

We designed and assembled a multi-stage launcher by stacking 6 coil assemblies end-to-end in a support housing which also aligns the system. Each coil is powered by its own capacitor bank which is triggered when an optical sensor in each stage determines that the projectile is in the firing position.

We are successfully demonstrating the induction launch technology for multi-stage systems. A 5 kg projectile can be accelerated from 12 m/s to 335 m/s with an average of 200 kJ stored in each of 6 stages. Calculations of launcher performance with our simulation code WARP-10 are in good agreement with experiments.

Acknowledgements

The authors thank Pace VanDevender, Sandia Director of Pulsed Power Sciences, and Bill Cowan, Manager of Advanced Energy Conversion Systems Department, for their enthusiastic support and for providing the opportunity to transform an idea to demonstration hardware. The authors thank the team of Robert Davis, Edward Ratliff, and Roque Feliciano in the design, fabrication, assembly, and operation of the launcher. The contributions of design definition by Bob Blackburn, development of the capacitor bank charging system by Ellis Dawson and Jim Majors of EG&G, coil fabrication by Tom Hesch and Meliton Gonzales, and spinner design by Dennis Muirhead are greatly appreciated.

References

[1] T. J. Burgess, *et al.*, "The Electromagnetic Theta Gun and Tubular Projectiles," Sandia National Laboratories Internal Report, SAND80-1988, Albuquerque, NM (1980).

[2] M. Cowan, *et al.*, "The Reconnection Gun," IEEE Transactions on Magnetics, Vol. 22, No. 6, (1986).

[3] M. Cowan, *et al.*, "Exploratory Development of the Reconnection Launcher, 1986-1989," presented at the 5th Symposium of Electromagnetic Launch Technology, Destin, Florida, April 2-5, 1990.

[4] Melvin M. Widner, "WARP-10: A Numerical Simulation Model for the Cylindrical Reconnection Launcher," presented at the 5th Symposium of Electromagnetic Launch Technology, Destin, Florida, April 2-5, 1990.

[5] Willard F. Hemsing, "Velocity sensing interferometer (VISAR) modification," Rev. Sci. Instrum., Vol. 50, No. 1, January, 1979.

[6] Billy W. Duggin, "Diagnostics and Firing Control for the Cylindrical Reconnection Launcher," presented at the 5th Symposium of Electromagnetic Launch Technology, Destin, Florida, April 2-5, 1990.

Induction Launcher Operation Sequence

1. Projectile approaches coil, input velocity measured

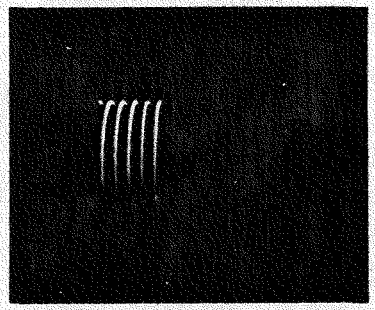

2. Start of current

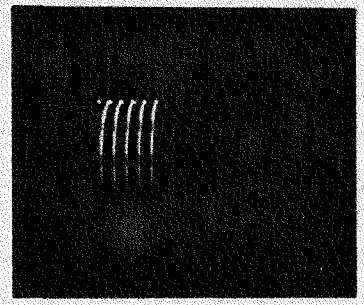

3. Projectile at peak acceleration

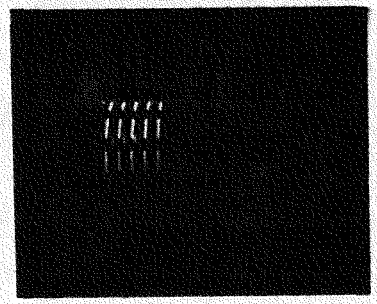

4. Projectile decoupled from coil

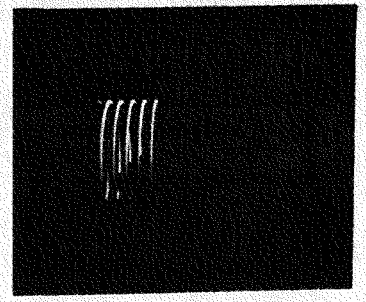

1

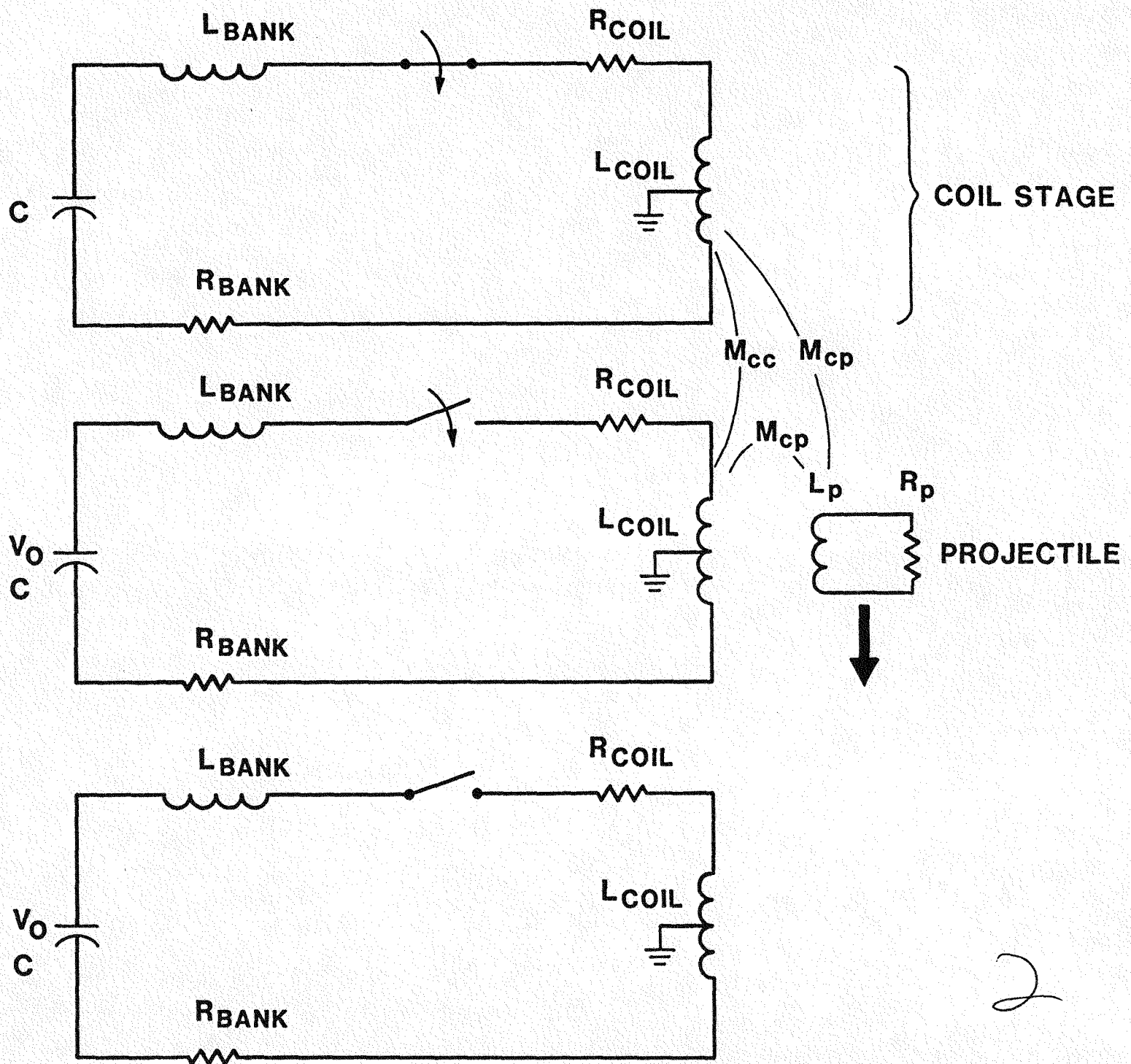
L BANK
R COIL
L COIL
C
R BANK
COIL STAGE
M cc
M cp
L BANK
R COIL
M cp
L p
R p
L COIL
V O
C
PROJECTILE
R BANK
L BANK
R COIL
L COIL
V O
C
R BANK

PRESSURE APPLIED TO FOURTH STAGE COIL WINDING AT PEAK CURRENT

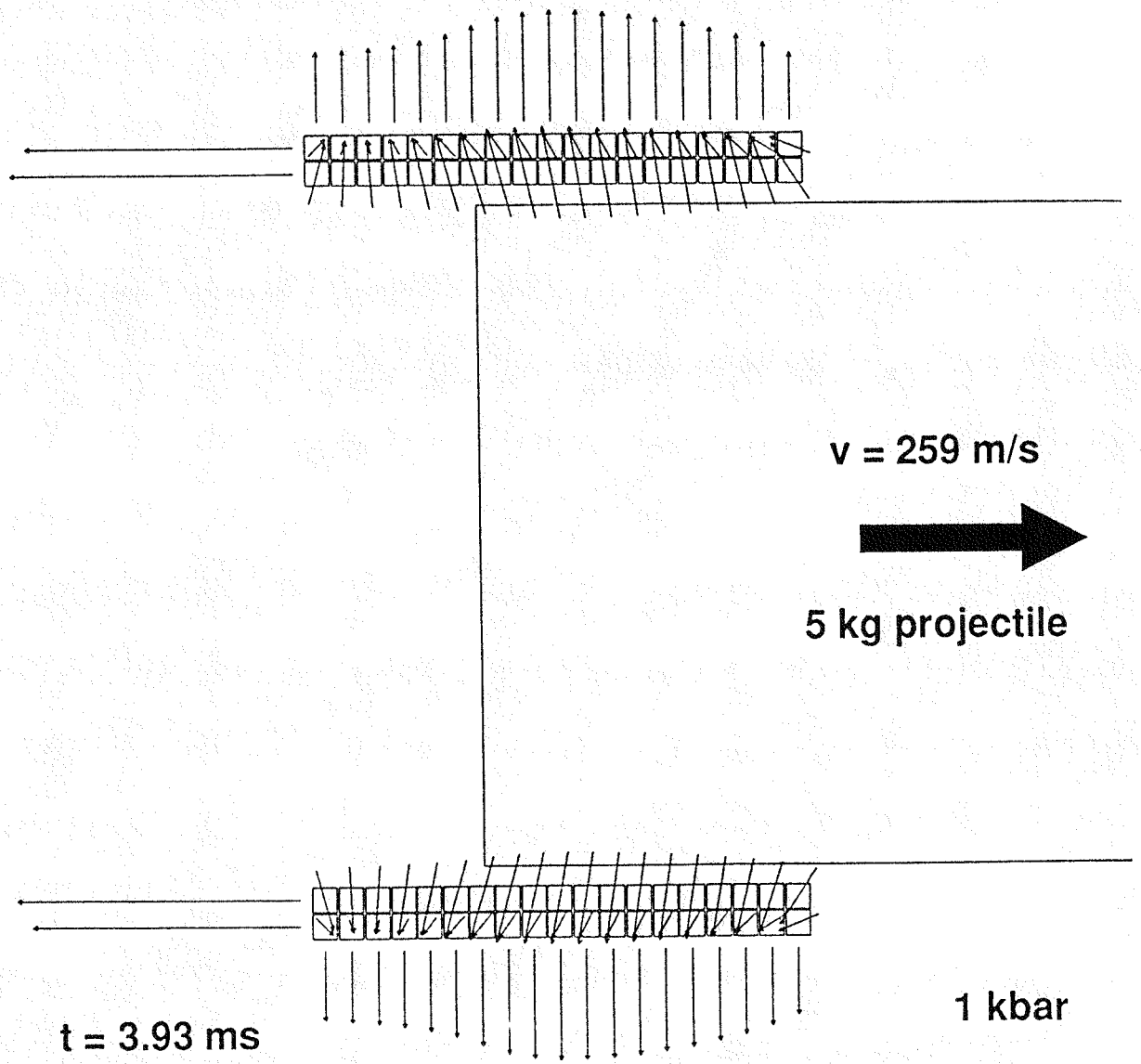

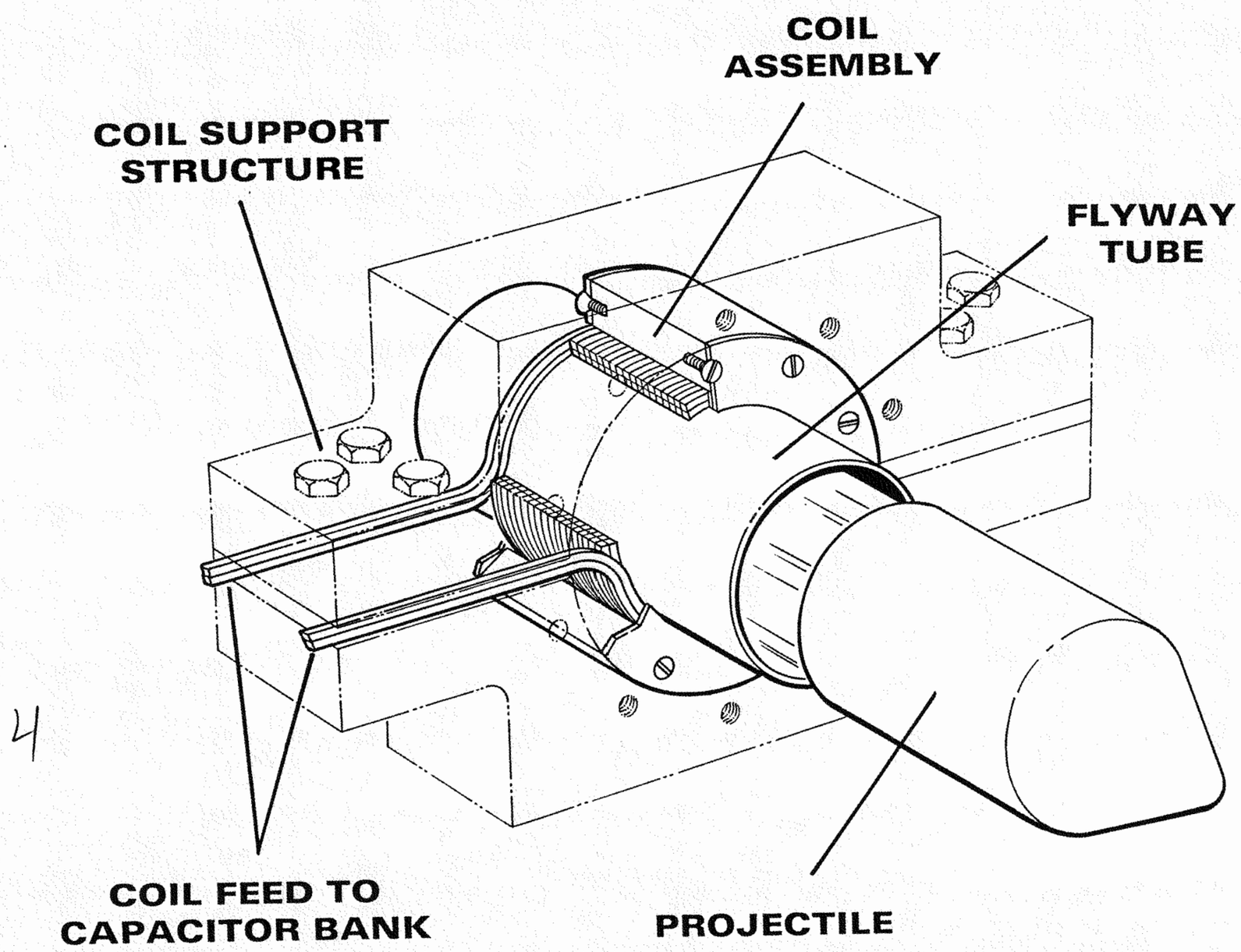
COIL
ASSEMBLY
COIL SUPPORT
STRUCTURE
FLYWAY
TUBE
COIL FEED TO
CAPACITOR BANK
PROJECTILE

4

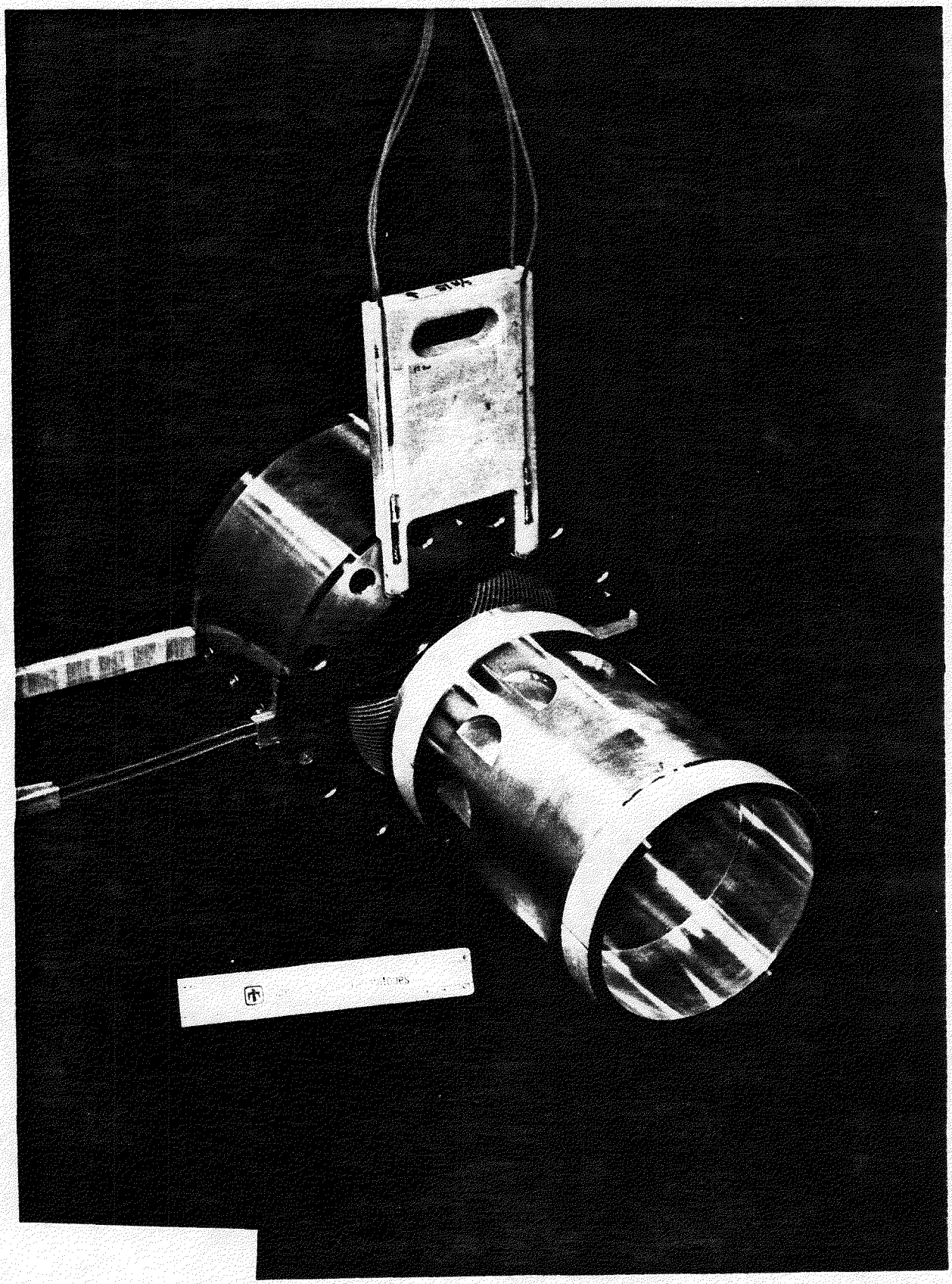

5

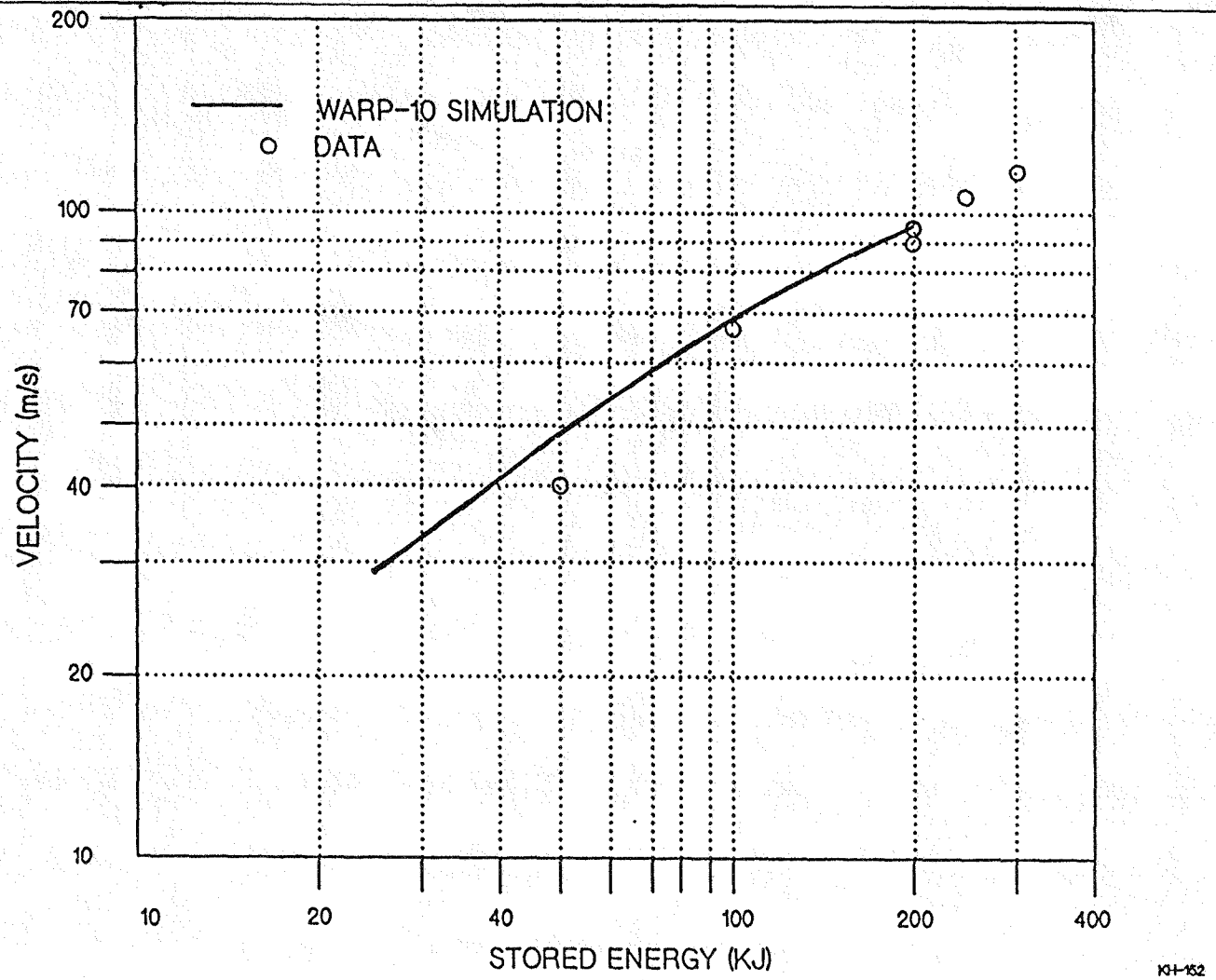
WARP-10 SIMULATION
DATA
VELOCITY (m/s)
200
100
70
40
20
10
10
20
40
100
200
400
STORED ENERGY (KJ)
KH-152

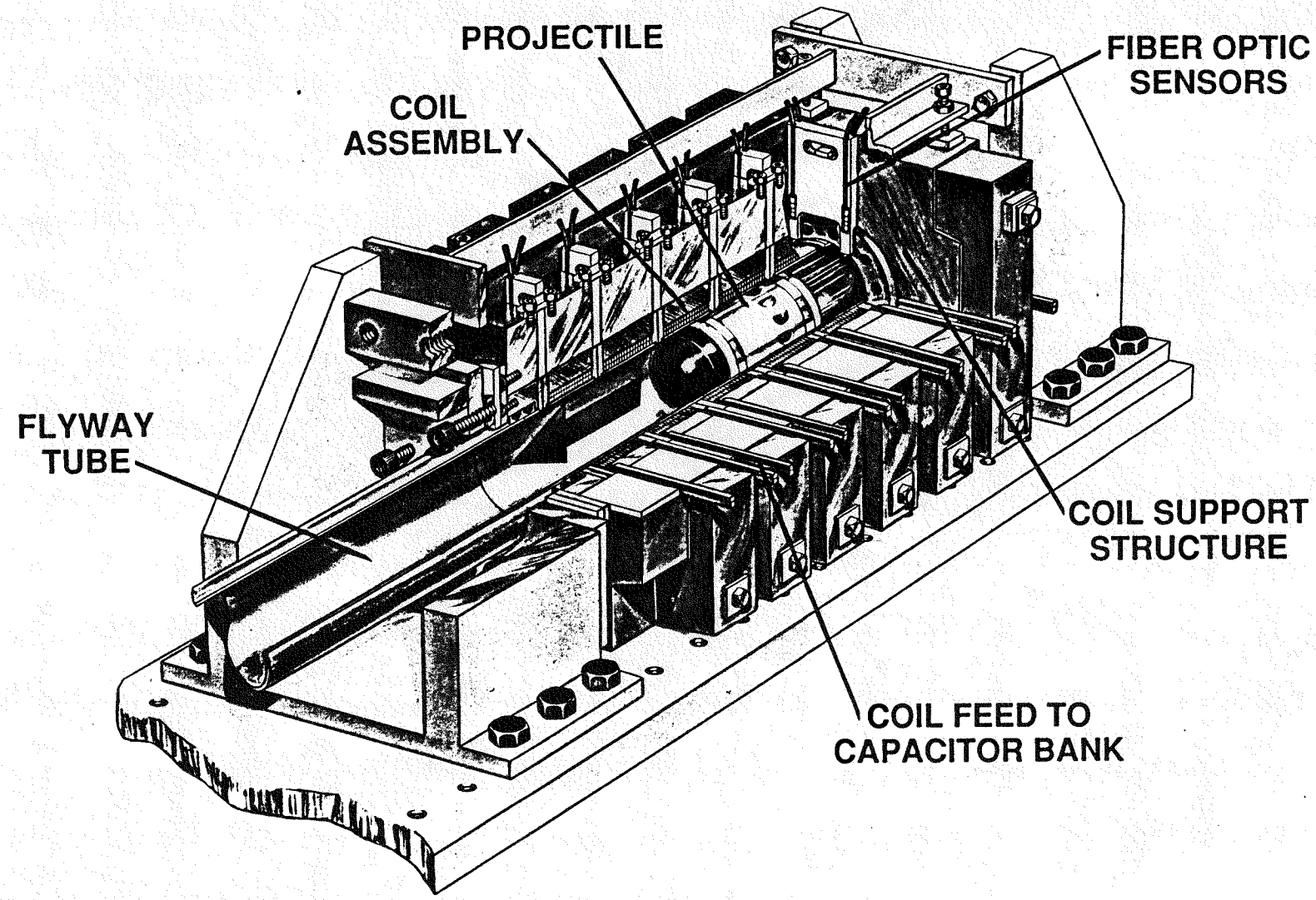

CUNNINGHAM
12/89

7

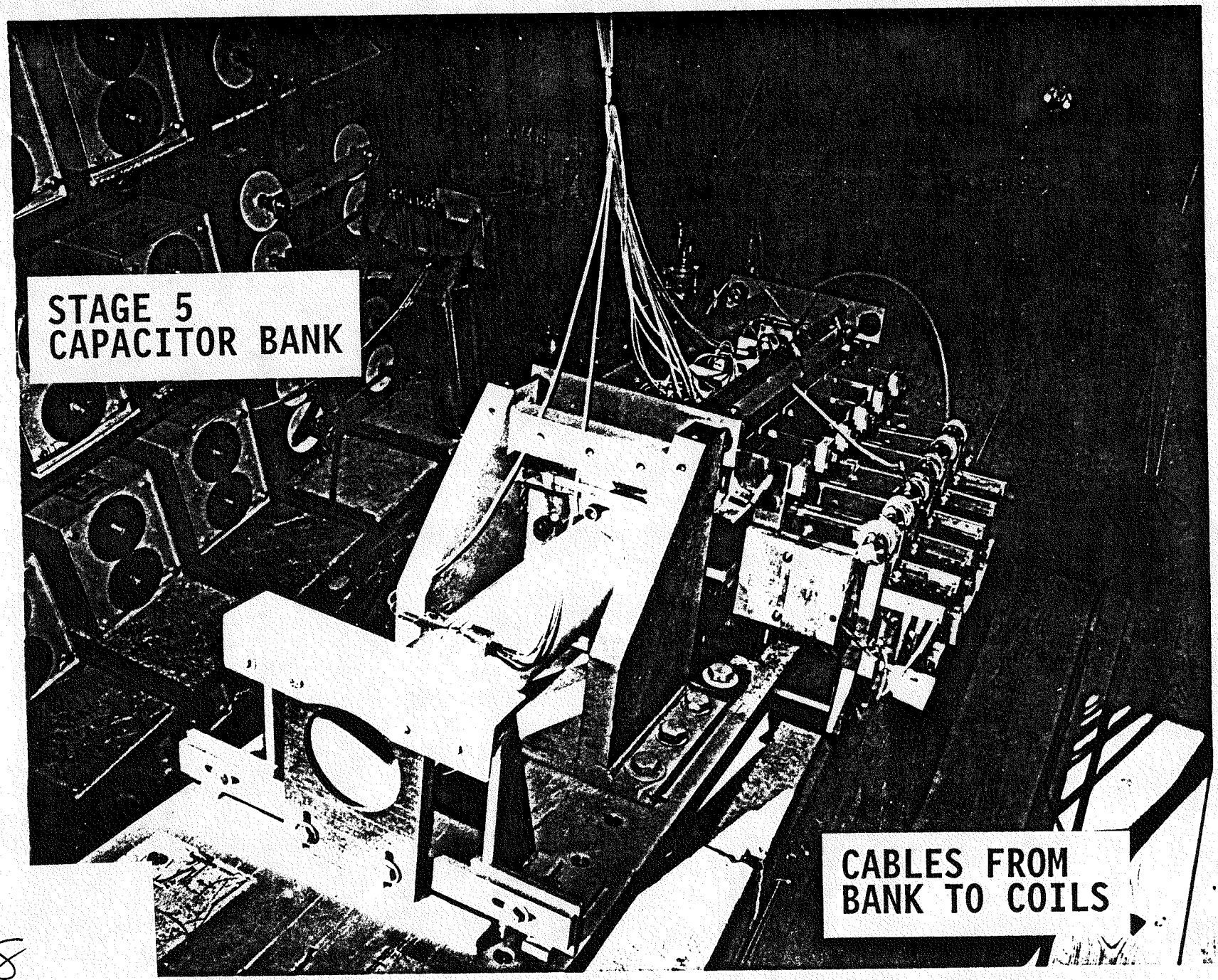
STAGE 5
CAPACITOR BANK
CABLES FROM
BANK TO COILS

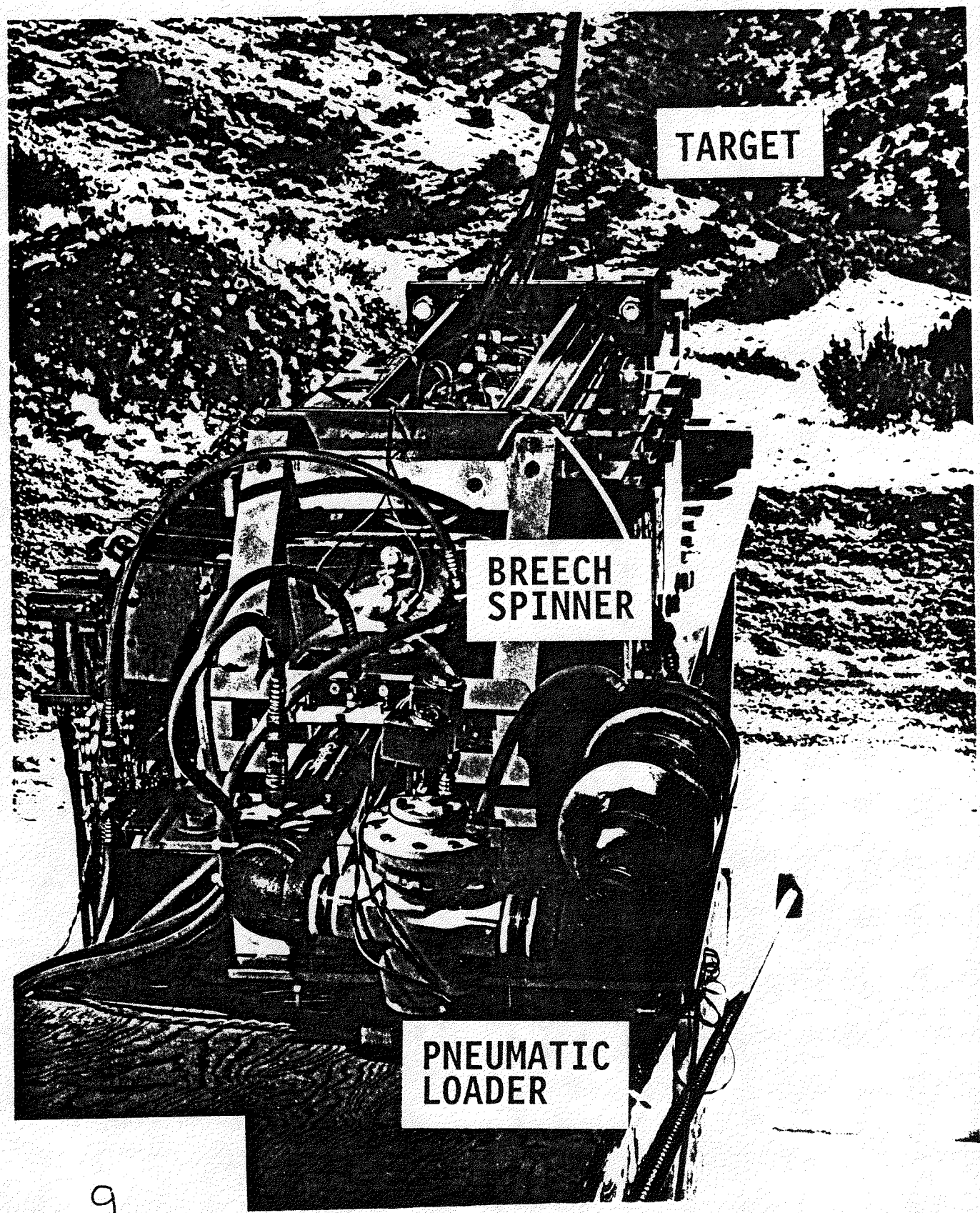
TARGET
BREECH
SPINNER
PNEUMATIC
LOADER

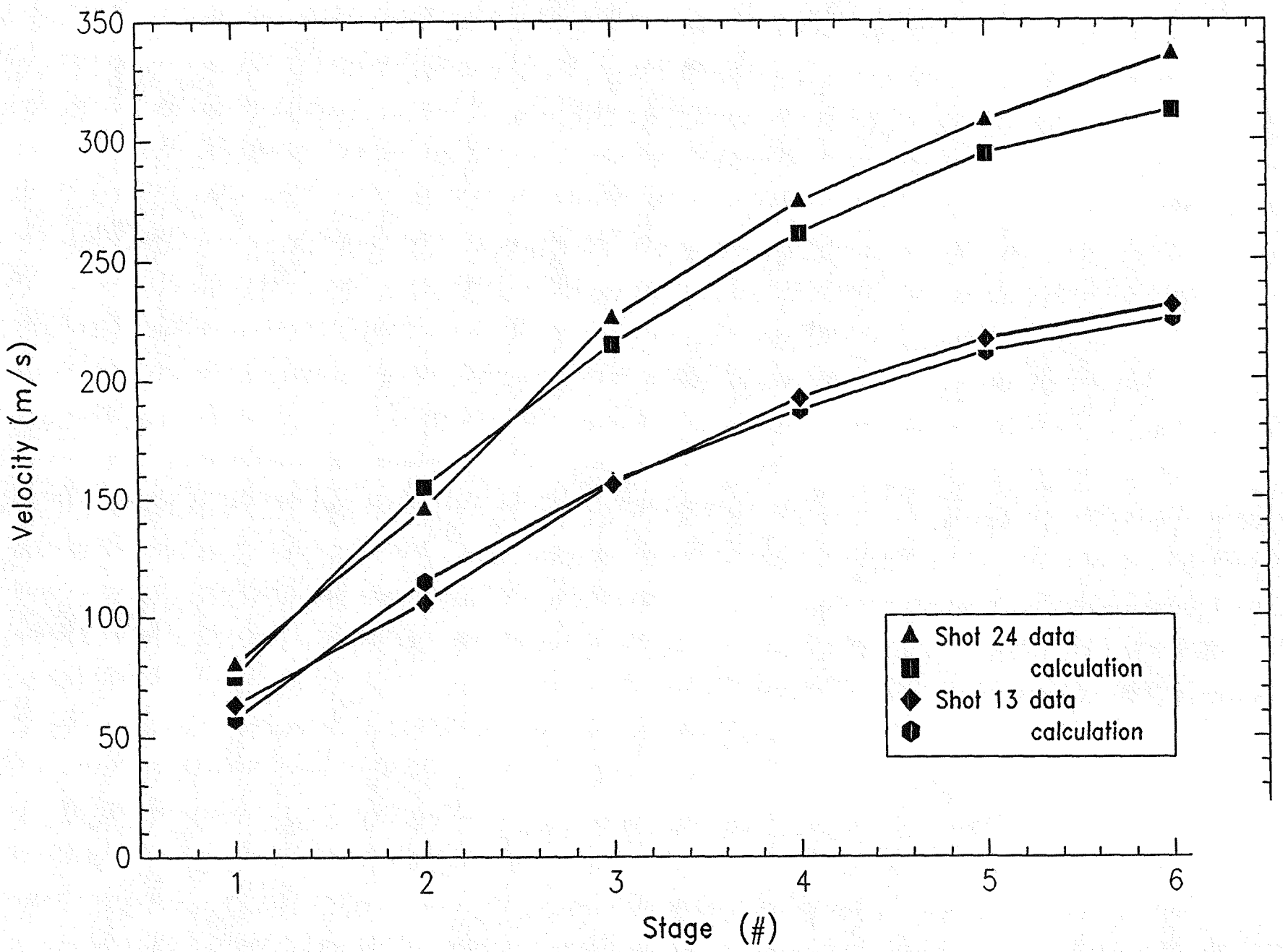
350
300
250
200
150
100
50
0
Velocity (m/s)
1
2
3
4
5
6
Stage (#)
Shot 24 data
calculation
Shot 13 data
calculation